

accreting hydrogen- and helium-rich gas from the disk onto a large rocky core (23). In Orion-like environments, there may not be time to grow the requisite cores before loss of the gas because Jupiter's formation would require 10^6 to 10^7 years. If giant planets form in Orion-like systems, they must do so before disk photoevaporation. One viable mechanism for rapid formation of giant planets is gravitational collapse, which has been modeled to occur in disks with $M_{\text{disk}} > 0.13 M_{\odot}$ on 10^3 -year time scales around solar-mass stars (24). Icy Kuiper belt objects and comets are believed to have formation time scales of 10^8 to 10^9 years (25). Thus, these objects are also difficult to form in Orion-like environments. The architectures of any new planetary systems that might form in Orion are likely to be different from that of our solar system.

The evidence for large particles in 114-426 complements several previous studies of particles in young disks. The reflected-light near-IR spectrum of the disk orbiting HR4796A (26) provides evidence for particles with radii larger than 2 to 3 μm . Several disks in NGC2024 (27) and Taurus (28) reveal relatively flat submillimeter spectra that may indicate large grains. However, near-IR observations of the disk in HH30 (29) show normal dust opacities and no evidence for grain growth, and sub-mm observations of the HL Tau disk (1) are inconclusive. Grain growth in disks appears to depend strongly on their environment.

The majority of young stars in the Milky Way Galaxy appear to have formed in large, dense clusters such as the Orion nebula, rather than in smaller, dark clouds such as Taurus-Auriga (4). Within large clusters, the majority of stars form near massive stars where their disks can be rapidly destroyed. Thus, planet formation models must be revised to consider the destructive effects of these environments. We present evidence for large grains in one Orion disk. This creates the possibility that planetary system with architectures different from our own solar system may nonetheless form in such hazardous environments.

References and Notes

1. S. V. W. Beckwith, T. Henning, Y. Nakagawa, in *Protostars and Planets IV*, V. Mannings, A. P. Boss, S. S. Russell, Eds. (Univ. of Arizona Press, Tucson, AZ, 2000), pp. 533–558.
2. C. J. Henney, C. R. O'Dell, *Astron. J.* **118**, 2350 (1999).
3. H. Stoerzer, D. Hollenbach, *Astrophys. J.* **495**, 853 (1998).
4. F. M. Walter, J. M. Alcalá, R. Neuhauser, M. Sterzik, S. J. Wolk, in *Protostars and Planets IV*, V. Mannings, A. P. Boss, S. S. Russell, Eds. (Univ. of Arizona Press, Tucson, AZ, 2000), pp. 273–298.
5. E. Churchwell, M. Felli, D. O. S. Wood, M. Massi, *Astrophys. J.* **321**, 516 (1987).
6. C. R. O'Dell, Z. Wen, X. Hu, *Astrophys. J.* **410**, 696 (1993).
7. M. J. McCaughrean, C. R. O'Dell, *Astron. J.* **111**, 1977 (1996).

8. M. J. McCaughrean *et al.*, *Astrophys. J.* **492**, L157 (1998).
9. J. Bally, C. R. O'Dell, M. J. McCaughrean, *Astron. J.* **119**, 2919 (2000).
10. D. Johnstone, D. Hollenbach, J. Bally, *Astrophys. J.* **499**, 758 (1998).
11. H. B. Throop, thesis, University of Colorado, Boulder (2000).
12. The term "interstellar" refers to the population of small, primordial dust grains in the Orion nebula that have not been processed in a circumstellar disk.
13. S.-H. Kim, P. G. Martin, P. D. Hendry, *Astrophys. J.* **422**, 164 (1994).
14. M. J. McCaughrean, K. R. Stapelfeldt, L. M. Close, in *Protostars and Planets IV*, V. Mannings, A. P. Boss, S. S. Russell, Eds. (Univ. of Arizona Press, Tucson, AZ, 2000), pp. 485–507.
15. K. Lumme, J. Rahola, J. W. Hovenier, *Icarus* **126**, 455 (1997).
16. M. I. Mishchenko, L. D. Travis, D. W. Mackowski, *J. Quant. Spec. Rad. Trans.* **55**, 535 (1996).
17. J. Bally, L. Testi, A. Sargent, J. Carlstrom, *Astron. J.* **116**, 854 (1998).
18. L. G. Mundy, L. W. Looney, E. A. Lada, *Astrophys. J.* **452**, L137 (1995).
19. H. Mizuno, W. J. Markiewicz, H. J. Voelk, *Astron. Astrophys.* **195**, 183 (1988).
20. M. S. Westley, R. A. Baragiola, R. E. Johnson, G. A. Baratta, *Nature* **373**, 405 (1995).
21. B. Dubrulle, G. Morfill, M. Sterzik, *Icarus* **114**, 237 (1995).
22. 114-426 is thought to show no photoevaporation because it is outside the Orion core's Strömgren sphere and thus receives no soft UV flux; we note the possibility that it may not be photoevaporating to-

- day because all gas has already been lost in previous photoevaporative episodes and it is a pure dust disk.
23. J. B. Pollack *et al.*, *Icarus* **124**, 62 (1996).
24. A. P. Boss, *Science* **276**, 1836 (1997).
25. P. Farinella, D. R. Davis, S. A. Stern, in *Protostars and Planets IV*, V. Mannings, A. P. Boss, S. S. Russell, Eds. (Univ. of Arizona Press, Tucson, AZ, 2000), pp. 1255–1282.
26. G. Schneider *et al.*, *Astrophys. J. Lett.* **513**, 127 (1999).
27. A. E. Visser, J. S. Richer, C. J. Chandler, R. Padman, *Mon. Not. R. Astron. Soc.* **301**, 585 (1998).
28. V. Mannings, J. P. Emerson, *Mon. Not. R. Astron. Soc.* **267**, 361 (1994).
29. A. M. Watson, K. R. Stapelfeldt, J. E. Krist, C. J. Burrows, in preparation.
30. J. A. Cardelli, G. C. Clayton, J. S. Mathis, *Astrophys. J.* **345**, 245 (1989).
31. H. Stoerzer, D. Hollenbach, *Astrophys. J.* **515**, 669 (1999).
32. H. W. Yorke, P. Bodenheimer, G. Laughlin, *Astrophys. J.* **411**, 274 (1993).
33. This research was funded by the Cassini project; the NASA Astrobiology Institute (grant NCC1-1052); NASA grants NAG5-8108, GO-07367.01-A, and GO-06824.01-A; Deutsches Zentrum für Luftund Raumfahrt (DLR) grant number 50-OR-0004; and European Commission Research Training Network RTN1-1999-00436. We thank C. Campbell, N. Turner, and two anonymous reviewers for their comments.

17 January 2001; accepted 20 April 2001
 Published online 26 April 2001;
 10.1126/science.1059093
 Include this information when citing this paper.

Observation of a Train of Attosecond Pulses from High Harmonic Generation

P. M. Paul,¹ E. S. Toma,² P. Breger,¹ G. Mullot,³ F. Augé,³ Ph. Balcou,³ H. G. Müller,^{2*} P. Agostini¹

In principle, the temporal beating of superposed high harmonics obtained by focusing a femtosecond laser pulse in a gas jet can produce a train of very short intensity spikes, depending on the relative phases of the harmonics. We present a method to measure such phases through two-photon, two-color photoionization. We found that the harmonics are locked in phase and form a train of 250-attosecond pulses in the time domain. Harmonic generation may be a promising source for attosecond time-resolved measurements.

The advent of subfemtosecond or attosecond (as) light pulses will open new fields of time-resolved studies with unprecedented resolution. Just as subpicosecond or femtosecond (fs) pulses have allowed the resolution of molecular movements, attosecond pulses may enable us to resolve electronic dynamics. Several groups around the world are researching the generation

of subfemtosecond pulses. Large bandwidths are required to support such pulses. The spectrum of a 200-as unipolar pulse covers the optical spectrum from the near infrared to the extreme ultraviolet. There are two known kinds of sources with the potential to produce coherent radiation over such bandwidths: high harmonic generation (HHG) (1) and stimulated Raman scattering (2, 3). Both methods have, in theory, a tendency to produce a train of closely spaced pulses rather than a single pulse. Even such trains of attosecond pulses, applied to experiments, can open a new field of attosecond physics, allowing the study of processes of unprecedented speed. Moreover, methods of selecting only one pulse from the train have already been suggested (4). The present experimental study focuses on HHG and demon-

¹Commissariat à l'Energie Atomique DRECAM/SPAM, Centre d'Etudes de Saclay, 91191 Gif-sur-Yvette, France. ²FOM-Institute for Atomic and Molecular Physics, Kruislaan 407, 1098 SJ, Amsterdam, Netherlands. ³Laboratoire d'Optique Appliquée, École Nationale Supérieure de Techniques Avancées (ENSTA)-Ecole Polytechnique, CNRS UMR 7639, 91761 Palaiseau Cedex, France.

*To whom correspondence should be addressed. E-mail: muller@amolf.nl

strates that this process indeed results in a train of attosecond pulses.

If an intense femtosecond laser pulse is focused on an atomic gas jet, the nonlinear electronic response of the medium causes the generation of higher harmonics of the laser field. The harmonic spectrum consists of a series of narrow peaks separated by twice the frequency of the driving field, and it extends far into the extreme ultraviolet regime (1). For reasons of symmetry, only odd harmonics are emitted. Although high harmonics have been a familiar presence in many laser laboratories for more than 10 years, and although their generation is well understood experimentally and theoretically (5–7), some features of the generation process have remained inaccessible to direct experimental measurement. In particular, questions relating to the time profile of the harmonic emission are not easily resolved. Measurements of the harmonic pulse duration show that it is much shorter than that of the driving laser (8–10) and lasts for only a few femtoseconds. In addition to questions related to the pulse envelope of an individual harmonic, another measurement difficulty involves beating between various harmonics; this occurs on a subfemtosecond time scale, and no streak camera or autocorrelator developed for this wavelength range can reach such a high resolution.

Theoretical results for the temporal characteristics of the generation process are much more detailed, and they predict that the harmonics are locked in phase. If this is correct, a group of neighboring harmonics could beat together to form a very short intensity spike, provided they all add constructively at the same instant. Because of the constant frequency spacing of the harmonics, this would happen twice per optical cycle of the driving laser. The duration of the spike could be as short as $T_{\text{laser}}/2N$ (where N is the number of phase-locked harmonics) (11, 12). At a laser wavelength of 800 nm, and $N = 5$, the output pulse would then be in the attosecond regime.

Numerical calculations for the single-atom response indicate that the harmonics are not emitted exactly in phase, leading to the generation of not one but several spikes per optical half-cycle (13). In practice, propaga-

tion of the electromagnetic fields through the medium affects the spatial and temporal coherence properties of the harmonic radiation. The theoretical conclusion is that per half-cycle only one of the interference spikes survives the propagation, thus forming a train of attosecond pulses spaced by half the period of the fundamental (13–15).

A recent experiment (16) has confirmed that the harmonic radiation contains structure on an attosecond scale. However, that experiment was based on measuring the field autocorrelate, which is equivalent to measuring the power spectrum of the harmonics; therefore, no information could be obtained about the relative phases of the harmonic components. It is exactly those phases that determine whether the harmonic field exhibits strong amplitude modulation (i.e., forms an attosecond pulse train), rather than being a frequency-modulated wave of approximately constant amplitude.

Our experiment approaches the problem from a direction closely related to the theoretical work of Veniard *et al.* (17). We seek to determine the phase relation between the contributing harmonics by considering them in pairs. The periodic beat pattern of such a pair can be related to the phase of the infrared (IR) light from the driving laser according to how the combined fields ionize atoms. The intensities of the individual harmonics are too weak to cause nonlinear effects on the target atoms, and thus only cause ionization by single-photon processes, each harmonic producing photoelectrons according to Einstein's equation for the photoelectric effect. The IR field, however, can easily be made to induce additional multiphoton transitions in the continuum (18). Ionization with a harmonic photon can then be accompanied by absorption as well as emission of different numbers of IR photons. In the electron spectrum, this results in the appearance of sidebands (Fig. 1).

At low IR intensities, where the problem can be treated in second-order perturbation theory, each harmonic has only a single sideband on each side. These sideband peaks appear at energies corresponding to even multiples of the IR photon energy, and are thus located between the peaks caused by the harmonics themselves. Only the two nearest

harmonics contribute to each sideband peak, each through two quantum paths (Fig. 2) that differ in the order in which the various photons are participating. According to Fermi's golden rule, the total transition probability from the initial ground state ψ_i , with energy E_0 , to all final states ψ_f (where f represents the angular quantum numbers of the continuum electron) at the sideband energy $E_q = E_0 + q\hbar\omega$ is proportional to $S = \sum_f |M_{f,q-1}^{(+)} + M_{f,q+1}^{(-)}|^2$, with $M_{f,q}^{(\pm)} = \langle \psi_f | D_{\text{IR}}^{\pm} (E_q - H)^{-1} D_q^+ + D_q^+ (E_{\pm 1} - H)^{-1} D_{\text{IR}}^{\pm} | \psi_i \rangle$. In these expressions, \hbar is Planck's constant divided by 2π , ω is the IR field frequency, H is the atomic Hamiltonian, the dipole operators D^+ correspond to the energy-increasing part of the electromagnetic perturbation,

$$E(t) \cdot r = D^+[\exp(-i\omega t)] + D^-[\exp(i\omega t)] \quad (1)$$

and their complex conjugates D^- to the energy-decreasing part (19). The IR field is present as D^- in $M_{f,q+1}^{(-)}$, because of the emission of the IR photon, and it thus contributes a phase of the opposite sign with respect to $M_{f,q-1}^{(+)}$. Explicitly writing the phases $D^{\pm} = D_0 \exp(\pm i\varphi)$, the interference terms in S become $A_f \cos(2\varphi_{\text{IR}} + \varphi_{q-1} - \varphi_{q+1} + \Delta\varphi_{\text{atomic}}^f)$, where $A_f = 2|M_{f,q-1}^{(+)}||M_{f,q+1}^{(-)}|$. Delaying the IR field by a time τ with respect to the harmonic fields sets $\varphi_{\text{IR}} = \omega_{\text{IR}}\tau$. By experimentally recording the magnitude of the sideband peak as a function of τ , and fitting a cosine to this, we determine $\varphi_{q-1} - \varphi_{q+1}$. The appearance of $\Delta\varphi_{\text{atomic}}^f$ is a consequence

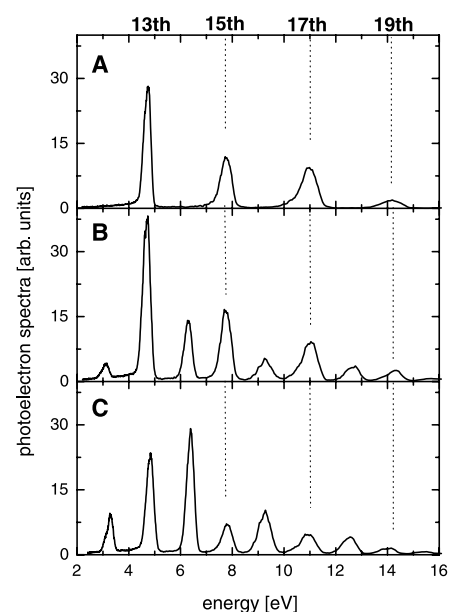


Fig. 1. Photoelectron spectra of argon ionized by a superposition of odd harmonics from an IR laser (A). In (B and C) copropagating fundamental radiation was added, causing sidebands to appear between the harmonic peaks. Changing the time delay between IR and harmonics from -1.7 fs in (B) to -2.5 fs in (C) causes a strong amplitude change of the sidebands.

Table 1. The atomic phases $\Delta\varphi_{\text{atomic}}^f$ and the relative strengths A_f of each two-photon transition responsible for the sideband peaks. The numbers within the parentheses represent the values of the angular and magnetic quantum numbers of the initial 3p state and the final continuum state of the listed energy.

Sideband	$\Delta\varphi_{\text{atomic}}^f$ (rad) / amplitude A_f (arbitrary units)			
	$(1,0) \rightarrow (1,0)$	$(1,0) \rightarrow (3,0)$	$(1, \pm 1) \rightarrow (1, \pm 1)$	$(1, \pm 1) \rightarrow (3, \pm 1)$
$E_0 + 12\hbar\omega$	0.438/6094	0.060/3659	0.125/1914	0.060/2440
$E_0 + 14\hbar\omega$	0.292/5135	0.102/2311	0.125/1281	0.102/1541
$E_0 + 16\hbar\omega$	0.221/3645	0.100/1349	0.108/763	0.100/899
$E_0 + 18\hbar\omega$	0.192/2444	0.090/742	0.090/427	0.090/494

REPORTS

of the intrinsic complex phase of the matrix elements (20, 21), resulting from $(E - H)^{-1}$ being applied at an energy in the continuous atomic spectrum (22). This phase is small and can be obtained from established theory with high precision (Table 1).

The experimental setup has been described in detail (9) and is shown in Fig. 2. At an intensity of ~ 100 TW/cm², many different odd harmonics are generated, but the tungsten mirror used to relay the beam into the electron spectrometer cuts off the spectrum beyond harmonic 19. The central part of the laser beam provides the IR light used to induce the sidebands, with adjustable phase (23). The spectrometer is observing an area with a radius of 125 μ m, located 1.5 mm before the focus of the spherical mirror. This was done to avoid the 180° phase slip that occurs when a light beam goes through a focus, and to ensure that the relative phase of the IR light and harmonics stays constant over the observed volume. The IR peak intensity can be estimated as <1 TW/cm², too weak to alter the photoelectron energies by ponderomotively shifting the ionization potential (9) (Fig. 1). This is also far below the threshold for multiphoton ionization of Ar by IR only.

The amplitudes of the first four sidebands, integrated over all corresponding energy

channels, are plotted as a function of the time delay τ in Fig. 3. Each point is divided by the total signal at that delay to compensate for fluctuations in the harmonic intensity (which, because of the high order of the generation process, is an extremely sensitive function of laser intensity). The curves are oscillating in phase with a periodicity of 1.35 fs (i.e., half of the IR field period). The good modulation depth (a factor of about 2) shows that the relative phases do not fluctuate too much over the beam profile, between shots, or within the profile of a single pulse. The oscillation period is that expected for the sideband interference, which is half of that expected for interference between IR components in the two beam parts. (The gas pressure in the harmonics jet was deliberately kept low to avoid contamination of the harmonics by scattered IR light.)

From the fitted pairwise phase differences, the phases of the involved harmonics (11 to 19) were found to be -2.6 , -1.3 , 0 , 1.8 , and 4.4 radians (24), respectively (arbitrarily assigning $\phi_{15} = 0$). Together with the relative harmonic intensities [obtained from Fig. 1A, corrected for the different ionization cross sections (25)], they uniquely determine the temporal intensity profile of the total field (Fig. 4). This profile is thus found to be a sequence of 250-as peaks [full width at half

maximum (FWHM)], spaced by 1.35 fs. Repeating this reconstruction several times with phases randomly modified according to the experimental standard error leads to similar results, with a standard deviation of 20 as in the FWHM pulse duration. The phase differences of the first four harmonics are close but not identical, so the resulting attosecond pulses will not be entirely bandwidth limited.

Provided the IR bandwidth is relatively small, our method in principle analyzes all individual frequency components within the harmonics bandwidth simultaneously and independently, with each part of the sideband

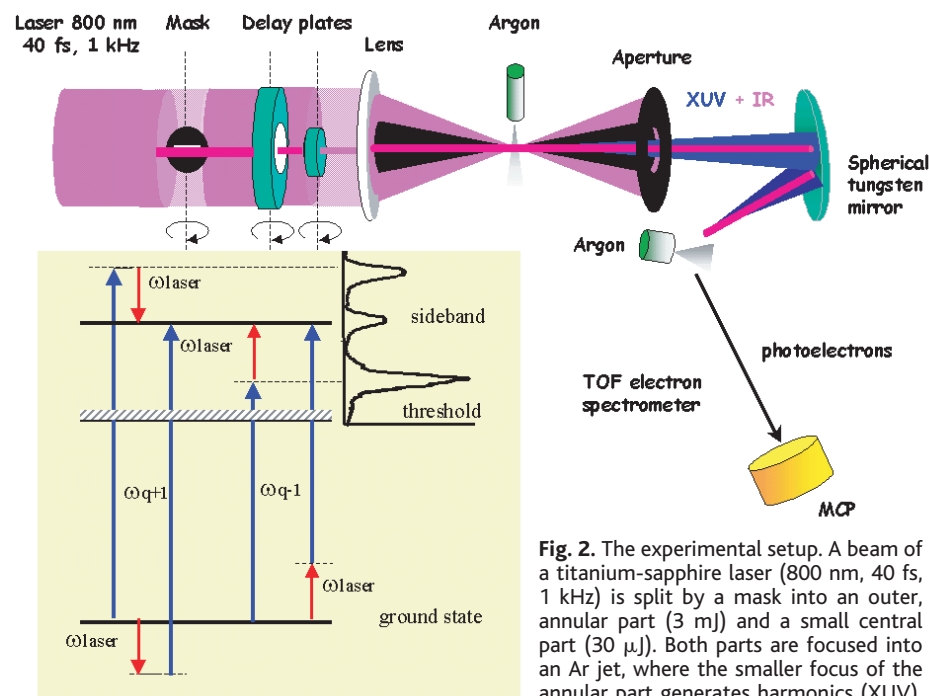


Fig. 2. The experimental setup. A beam of a titanium-sapphire laser (800 nm, 40 fs, 1 kHz) is split by a mask into an outer, annular part (3 mJ) and a small central part (30 μ J). Both parts are focused into an Ar jet, where the smaller focus of the annular part generates harmonics (XUV). The annular part is then blocked by a

pinhole, and only the central part of the IR pulse and its harmonics propagates into a magnetic-bottle spectrometer. The light is refocused there by a spherical tungsten-coated mirror (focal length 35 mm) onto a second Ar jet, and the electrons resulting from photoionization in this jet are detected at the end of the time-of-flight (TOF) tube by microchannel plates (MCP). The harmonics and IR pulse can be delayed with respect to each other by using antireflection-coated glass plates (6 mm thick) cut from the same window. The inset shows the quantum paths contributing to the photoelectrons generated in the second argon jet by mixed-color two-photon ionization; ω_{laser} is the IR field frequency and ω_q equals $q\omega_{\text{laser}}$

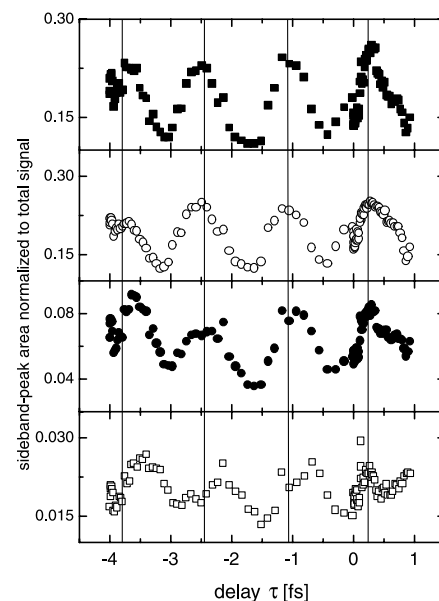


Fig. 3. Area of the first four sideband peaks (to higher energies from top to bottom) as a function of the time delay between the IR pulse and the harmonics. The first three curves oscillate in phase; the lowest one is shifted forward by 0.35 fs. The vertical lines are spaced by 1.35 fs, half the cycle time of the driving laser.

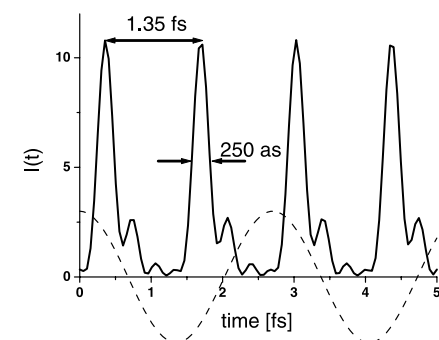


Fig. 4. Temporal intensity profile of a sum of five harmonics, as reconstructed from measured phases and amplitudes. The FWHM of each peak is ~ 250 as. The cosine function represents the IR probe field for zero delay. Note that this reconstruction recovers “typical” properties of pulses in the train by assuming all pulses are identical; in reality the pulse properties might have some variation around this “average.”

peak responding to the two frequency components that contribute to it. The sideband peak profile will thus show modulation with τ if phase differences vary over the bandwidth. Such profile changes are not apparent in our data, hence the harmonics must be frequency-modulated (“chirped”) in a similar way. An identical chirp in all harmonics does not affect the intensity envelope of the attosecond pulses, only the phase of their carrier wave (which we cannot measure).

The experimental evidence presented here for the existence of attosecond pulses in the process of HHG confirms theoretical predictions that the natural phase with which groups of neighboring harmonics are generated is sufficient to cause such pulse trains. In addition, our technique of phase measurement is a general one, applicable to deep in the extreme ultraviolet, and scales without difficulty to larger groups of harmonics. A measurement scheme for the phases may enable their purposeful manipulation (e.g., through dispersion when propagating through a gas cell), even if the harmonics were initially generated with undesirable phases. With such techniques, it should ultimately become possible to properly phase all harmonics emerging from the generation jet, leading to pulses perhaps as short as 10 as. The generation of these pulses still must be investigated in more detail, and ways of control and selection must be developed, before attosecond pulses can be routinely used as light sources in experiments.

References and Notes

1. P. Salières, A. L’Huillier, P. Antoine, M. Lewenstein, in *Advances in Atomic, Molecular, and Optical Physics*, B. Bederson, H. Walther, Eds. (Academic Press, New York, 1999), vol. 41, p. 83.
2. A. E. Kaplan, *Phys. Rev. Lett.* **73**, 1243 (1994).
3. A. V. Sokolov, D. R. Walker, D. D. Yavuz, G. Y. Yin, S. E. Harris, *Phys. Rev. Lett.* **85**, 562 (2000).
4. M. Ivanov, P. B. Corkum, T. Zuo, A. Bandrauk, *Phys. Rev. Lett.* **74**, 2933 (1995).
5. P. B. Corkum, *Phys. Rev. Lett.* **71**, 1994 (1993).
6. M. Lewenstein, P. Balcou, M. Ivanov, A. L’Huillier, P. B. Corkum, *Phys. Rev. A* **49**, 2117 (1994).
7. W. Becker, A. Lohr, M. Kleber, M. Lewenstein, *Phys. Rev. A* **56**, 645 (1997).
8. T. Sekikawa, T. Ohno, T. Yamazaki, Y. Nabekawa, S. Watanabe, *Phys. Rev. Lett.* **83**, 2564 (1999).
9. E. S. Toma et al., *Phys. Rev. A* **62**, 061801(R) (2000).
10. M. Drescher et al., *Science* **291**, 1923 (2001).
11. G. Farkas, C. Toth, *Phys. Lett. A* **168**, 447 (1992).
12. S. E. Harris et al., *Opt. Commun.* **100**, 487 (1993).
13. P. Antoine, A. L’Huillier, M. Lewenstein, *Phys. Rev. Lett.* **77**, 1234 (1996).
14. P. Antoine et al., *Phys. Rev. A* **56**, 4960 (1997).
15. I. P. Christov, M. M. Murnane, H. C. Kapteyn, *Phys. Rev. A* **57**, 2285 (1998).
16. N. A. Papadogiannis, B. Witzel, C. Kalpouzos, D. Charalambidis, *Phys. Rev. Lett.* **83**, 4289 (1999).
17. V. Veniard, R. Taieb, A. Maquet, *Phys. Rev. A* **54**, 721 (1996).
18. J. M. Schins et al., *J. Opt. Soc. Am. B* **13**, 197 (1996).
19. The rotating-wave approximation is used.
20. S. Klarsfeld, A. Maquet, *J. Phys. B* **12**, L553 (1979).
21. M. Aymar, M. Crance, *J. Phys. B* **13**, L287 (1980).
22. The turn-on boundary condition prescribes in ω_0 an infinitesimal positive imaginary part $i\eta$, which defines the integral in the spectral representation of $(E - H)^{-1}$ as a (real) principal-value integral minus an imaginary delta function $i\pi\delta(E - H)$.

23. The plates could be aligned parallel with each other within a precision of 0.01°. The path of any of the beams through its plate depends on the incidence angle, which can be changed by rotating the plate. The plate responsible for the delay of the central part of the beam is mounted on a computer-controlled rotation stage, which can make steps of 0.005°. Very small delays can be achieved with it, because close to the normal incidence, the time delay has second-order dependence on the incidence angle. Given the dimensions of our plates, a tilt of 1° produces a delay of 1 fs of the pulse.
24. The standard deviation in these phases is about 0.3 radian.
25. The amplitude of the 11th harmonic was not directly measured. Because the modulation depths of all side-

bands are similar, we can conclude that harmonic 11 is not much different from harmonic 13 in intensity. In the calculations we used a value 1.5 times that of the 13th-harmonic magnitude. Had this ratio been 0.5, the peak FWHM in Fig. 4 would have been only slightly longer.

26. This work is part of the research program of FOM (Fundamental Research on Matter), which is subsidized by NWO (Netherlands Organization for the Advancement of Research). It was also supported by the European Commission (Access Contract HPRI-CT-1999-00086) and by the EC’s Training and Mobility of Researchers program (contract HPRN-CT-2000-00133). We thank V. Veniard, R. Taieb, A. Maquet, and E. Constant for useful discussions.

30 January 2001; accepted 20 April 2001

Anomalous Weak Magnetism in Superconducting $\text{YBa}_2\text{Cu}_3\text{O}_{6+x}$

J. E. Sonier,^{1,3*} J. H. Brewer,^{2,3} R. F. Kiefl,^{2,3} R. I. Miller,² G. D. Morris,³ C. E. Stronach,⁴ J. S. Gardner,⁵ S. R. Dunsiger,^{2†} D. A. Bonn,² W. N. Hardy,² R. Liang,² R. H. Heffner⁶

For some time now, there has been considerable experimental and theoretical effort to understand the role of the normal-state “pseudogap” phase in underdoped high-temperature cuprate superconductors. Recent debate has centered on the question of whether the pseudogap is independent of superconductivity. We provide evidence from zero-field muon spin relaxation measurements in $\text{YBa}_2\text{Cu}_3\text{O}_{6+x}$ for the presence of small spontaneous static magnetic fields of electronic origin intimately related to the pseudogap transition. Our most significant finding is that, for optimal doping, these weak static magnetic fields appear well below the superconducting transition temperature. The two compositions measured suggest the existence of a quantum critical point somewhat above optimal doping.

Of the high-temperature cuprate superconductors, $\text{YBa}_2\text{Cu}_3\text{O}_{6+x}$ has been the most widely studied. The parent compound, $\text{YBa}_2\text{Cu}_3\text{O}_6$, is an antiferromagnetic (AF) insulator that becomes a superconductor with hole (oxygen) doping. Nuclear magnetic resonance (NMR) (1), inelastic neutron scattering (2), and muon spin relaxation (μSR) (3–6) studies clearly show that short-range AF correlations of the Cu spins in the CuO_2 planes persist for hole concentrations well beyond the three-dimensional AF phase, leading some to suspect a spin-fluctuation pairing mechanism for superconductivity. Recently, the onset of spin fluctuations above the superconducting transition tem-

perature T_c has been linked to the formation of the pseudogap (7), first observed (8) as a gap in the spin-excitation spectrum of $\text{YBa}_2\text{Cu}_3\text{O}_{6.7}$ and later identified as a coinciding gap in the quasiparticle-excitation spectrum (9). Early interpretations of the pseudogap favored a scenario in which phase-incoherent pairing correlations (10), established in the normal state at a crossover temperature T^* , condense into the coherent superconducting state below the transition temperature T_c . Experiments showing that the pseudogap above T_c evolves continuously into the superconducting gap below T_c lent strong support to this idea. However, a careful examination by Tallon and Loram (11) of several key experiments supports an alternative view, whereby the pseudogap is in fact distinct from the superconducting gap, and the temperature T^* defines an energy scale that vanishes ($T^* \rightarrow 0$) in the slightly overdoped region at a critical point $p_{cr} \approx 0.19$ (where p is the fraction of holes per Cu atom in the CuO_2 plane). A crucial observation is that short-range AF correlations persist at temperatures above 0 K at the critical hole concentration $p_{cr} = 0.19$.

Consistent with the latter view, several groups have proposed that there is another source of magnetism, which is distinct from the Cu-spin magnetism and more intimately asso-

¹Department of Physics, Simon Fraser University, Burnaby, British Columbia V5A 1S6, Canada. ²Department of Physics and Astronomy, University of British Columbia, Vancouver, British Columbia V6T 1Z1, Canada. ³TRIUMF, Vancouver, British Columbia V6T 2A3, Canada. ⁴Department of Physics, Virginia State University, Petersburg, VA 23806, USA. ⁵National Research Council, Chalk River, Ontario K0J 1P0, Canada. ⁶Los Alamos National Laboratory, Los Alamos, NM 87545, USA.

*To whom correspondence should be addressed. E-mail: jeff_sonier@sfu.ca

†Present address: Department of Physics and Astronomy, University of California Los Angeles, Los Angeles, CA 90095, USA.